

Angle based dynamic learning rate for gradient descent

Neel Mishra

CSTAR

IIT Hyderabad

Hyderabad, India

neel.mishra@research.iiit.ac.in

Pawan Kumar

CSTAR

IIT Hyderabad

Hyderabad, India

pawan.kumar@iiit.ac.in

Abstract—In our work, we propose a novel yet simple approach to obtain an adaptive learning rate for gradient-based descent methods on classification tasks. Instead of the traditional approach of selecting adaptive learning rates via the decayed expectation of gradient-based terms, we use the angle between the current gradient and the new gradient: this new gradient is computed from the direction orthogonal to the current gradient, which further helps us in determining a better adaptive learning rate based on angle history, thereby, leading to relatively better accuracy compared to the existing state-of-the-art optimizers. On a wide variety of benchmark datasets with prominent image classification architectures such as ResNet, DenseNet, EfficientNet, and VGG, we find that our method leads to the highest accuracy in most of the datasets. Moreover, we prove that our method is convergent.

Index Terms—Adam, Image Classification, Optimization, Angle, Gradient Descent, Neural Networks, ResNet

I. INTRODUCTION

Stochastic gradient methods have become increasingly popular in various fields due to their effectiveness in optimizing large-scale problems and handling noisy data. In machine learning, they are extensively used to train deep learning models, such as neural networks, where they enable efficient optimization of high-dimensional, non-convex loss functions. Stochastic gradient descent (SGD) and its variants have been the cornerstone of training deep learning models in areas like computer vision, natural language processing [10], [29], [42], and reinforcement learning [19], [40]. Additionally, stochastic optimization techniques have been adapted for online and distributed learning, facilitating real-time adaptation and scalability to massive datasets in applications like recommendation systems [5], [30] and search engines.

Although the popular stochastic gradient descent (SGD) is a simple method and is known to have a convergence to local minima with a small enough learning rate, it doesn't give better results compared to modern optimizers in deep learning architectures. The vanilla SGD uses the same learning rate for the entire training process and incorporates very little curvature information, leading it to get stuck to a local optimum.

Recent approaches have tried to overcome the oscillations associated with SGD with the help of momentum [39], authors in [32] have argued that the reason momentum speeds up the

convergence is that it brings some eigen components of the system closer to critical damping.

Although momentum can deal with the oscillations in training, the problem of fixed learning rate is not addressed solely by momentum. There have been many works in the literature to address the static learning rate [35]; the Rprop algorithm [33] had tried to accomplish a dynamic learning step for full batch gradient descent by increasing and decreasing the step size of a particular weight corresponding to the sign of the last two gradients. If the signs are opposite, then that indicates deviation, and hence the learning rate is decremented, and if the sign is positive, then the learning rate is incremented. Hence, the step size is adapted for every iteration.

Another branch of optimizers like Nesterov Accelerated Gradient (NAG) [31] include those that try to correct the gradient using the momentum to form a look-ahead vector. From this look-ahead, they see the direction of the gradient at that point, and subsequently, use that gradient to perform the weight updates from the previous point.

Adagrad [9] tries to use the expectation of the square of the gradients to scale the gradient element-wise, but it failed to learn after some epochs as the summation keep growing during the training. An extension to Adagrad is the algorithm Adadelta [46]; instead of just accumulating gradients, they use a decaying average of past updates, alongside exponentially decaying average of gradients. The method RMSProp [13], which was introduced in a lecture as a mini-batch version of RProp, also uses an exponentially decaying average of gradients, but it differs from Adadelta because it doesn't use the exponentially decaying average of past updates; however, the first update of Adadelta is same as that of RMSProp.

Another recently popular optimizer Adam [20], can be thought of as a combination of momentum and RMSprop. Adam incorporates gradient scaling witnessed in RMSprop and use momentum via the moving average of gradients to tackle oscillations. It also includes bias corrections.

Authors in [8] introduce a friction coefficient called diffGrad friction coefficient (DFC); They compute this coefficient using a non-linear sigmoid function on the change in gradients of current and immediate past iteration. Adabelief [47], another popular optimizer uses the square of the difference between the current gradient and the current exponential moving average to

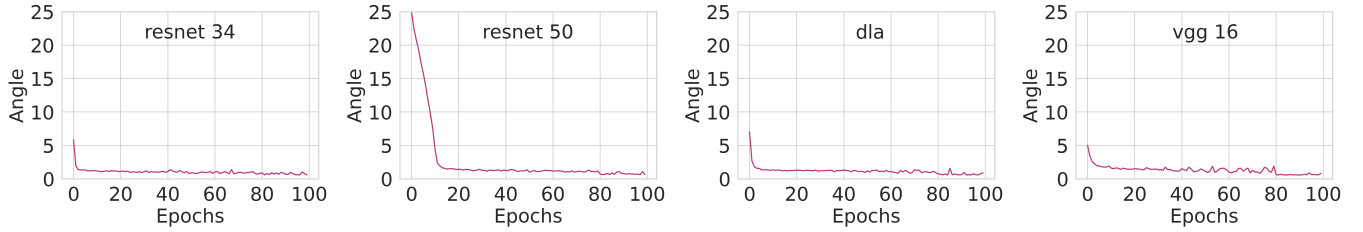


Fig. 1: Progression of angles with increasing epochs on CIFAR 10 dataset. We observe that for most of the architectures, except of epochs less than 10, the angles are between 0-2 degrees. This is configured in such a way because too less of an angle and the cot becomes unstable, and attempting to have larger angles by having a larger h can lead to g_1 and g_2 (See Figure 1) in the algorithm 1, to lie in different localities.

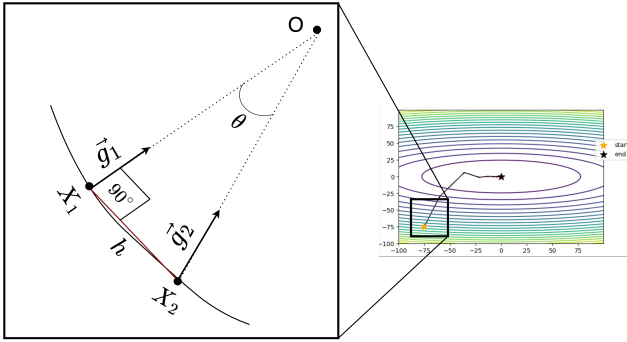


Fig. 2: Illustration of one iteration of the proposed method.

scale the current gradient. Many of the popular optimizers have played around with these four properties, namely, momentum, a decaying average of gradients or weight updates, gradient scaling, and a lookahead vector to derive their gradient update rules.

There have been few papers that have considered the angle information between successive gradients. The authors in [38] try to correct the obtained gradient by using the angle between the successive current and the past gradients. The authors in [34] have also used the angle between successive gradients. They control the step size based on the angle obtained from previous iterations and use it to calculate the angular coefficient, essentially the \tanh of the angle between successive gradients. They claim that it reduces the oscillations between the successive gradient vectors; they also combine the gradient scaling, like RMSprop, and the expected weighted average of gradients as in ADAM.

Other notable optimization methods which are variants of Adam for deep learning are NADAM [7], Rectified Adam (RAdam) [28], Nostalgic Adam [15], and AdamP [12]. Preconditioning gradient methods are usually popular to accelerate the convergence of gradient methods [1], [3], [4], [18], [24]–[27], [36] for solving large sparse linear systems stemming from scientific computing applications. Similar preconditioned stochastic gradient methods have been tried [2], [22], but they are not as effective.

In this paper, we propose a simple technique for estimat-

ing an adaptive learning rate for SGD. The learning rate is obtained by determining the angle between the current gradient g_1 computed at the current location x_1 and a new probing gradient g_2 computed at a new location x_2 , which is at an orthogonal distance from the current location. This angle is then used to determine an effective learning rate (See Algorithm 1 for details). A graphical illustration of our method is shown in Figure 2.

A. Our Contributions

We summarize our contributions as follows:

- 1) We propose a dynamic learning rate for vanilla SGD. Our method uses a geometric approach, which is simple, easy to implement, and very effective.
- 2) We show that under certain assumptions the proposed method is convergent and satisfies the well-known Armijo's condition for sufficient decrease.
- 3) We show an extensive set of accuracy results and comparisons of prominent stochastic optimization solvers on various image classification architectures and prominent datasets.

II. THE PROPOSED METHOD

To facilitate an adaptive and more accurate step size, we consider a snapshot in the global gradient vector field, it is well known that the gradient vectors will be perpendicular to the tangential plane of the level curve at each point of the vector field. The existing gradient descent methods go parallel to the negative gradient g_1 from the point X_1 , instead, we first go perpendicular in the direction of g_1^\perp towards a new point X_2 by a small h step (a hyperparameter); the direction g_1^\perp is any random vector inside the tangential plane. At X_2 we calculate another negative gradient g_2 . Let point O be the intersection point of these two gradients. We now simply use these information to calculate the height of the triangle as shown in the Figure 2 by calculating the step size $d = h \cdot \cot(\theta)$ in the step 8 of the Algorithm 1, where θ is the angle between the two vectors g_1 and g_2 . We then travel in the direction of normalized g_1 with step size d as shown in step 13 of the algorithm 1, and essentially reach the intersection point O of the two gradients; we repeat this process until convergence.

Although the perpendicular step size is fixed and static, our learning rate changes with every new iteration. The perpendicular step h plays a critical role in our method; too large of a perpendicular step will lead g_1 and g_2 to point to different localities in non-convex settings. Hence, the calculation of step length will make no sense. On the other hand, if the value of h is too small, then the gradient vectors will overlap, and the angle between these gradients will be too small to compute precisely. So to tackle this issue, we keep a relatively small perpendicular step size h , and we add some ϵ to h because $\cot \theta$ is infinite when θ is zero. Figure 1 shows the resulting angle for the optimal h on different architectures. In steps 8 to 11 of algorithm 1, we use the decayed expectation (step 9) of the step size to double the current estimated step size (step 11), if the current estimated step size is lesser than the expected step size.

Algorithm 1 Our Method

Input: X

Parameter: h, β

```

1: while not converged do
2:    $X_1 \leftarrow X$                                  $\triangleright$  Initial random guess
3:    $g_1 \leftarrow -\nabla_X f(X_1)$ 
4:    $p_1 \leftarrow g_1^\perp$                            $\triangleright$  Perpendicular unit vector to  $g_1$ 
5:    $X_2 \leftarrow X_1 - h \cdot p_1$ 
6:    $g_2 \leftarrow -\nabla_X f(X_2)$ 
7:    $\theta \leftarrow \angle(g_1, g_2) + \epsilon$ 
8:    $d \leftarrow h \cdot \cot \theta$                        $\triangleright$  Find current step size
9:    $d_{avg} \leftarrow \beta \cdot d_{avg} + (1 - \beta) \cdot d$      $\triangleright$  Average step size
10:  if  $d < d_{avg}$  then
11:     $d \leftarrow 2 \cdot d$ 
12:  end if
13:   $X \leftarrow X_1 + d \cdot \frac{g_1}{\|g_1\|}$            $\triangleright$  Update step
14: end while

```

III. EXPERIMENTS ON SOME TOY EXAMPLES

In this section, we experimentally demonstrate the potential of our method to overcome bad minima; for this, we have crafted two challenging surfaces using the tool [16]. We have also shown the 3D visualization for the same in Figures 3a and 4a. For the experimental setup on these toy examples, we set the learning rate $\eta = 1e-2$, we keep the same initial point for all the methods, and we train them up to 1000 iterations.

A. Toy Example A

In the toy example A, we consider the following simple function

$$f(x, y) = -y^2 \sin x. \quad (1)$$

We see in Figure 3a that the surface corresponding to this function is wavy and has multiple local minima. The initialization point is $(-2.0, 0.0)$ as shown in the Figure 3a. Although our trajectory is the same as that of SGD without momentum, we can see that while all the optimizers get stuck at the relatively bad local minima, our proposed optimizer goes to a better local

minimum, and it doesn't stop there; we can see that it tries to go further only to come back due to steep curvature ahead. Even though the gradient amplitude may be small in a region, since we take the unit direction of gradient to estimate the perpendicular direction, this perpendicular step is invariant to the current gradient amplitude. Hence, it can explore a region where the gradient is more substantial and use it to estimate an effective step length that may lead to further descent.

B. Toy Example B

The toy example B is defined as follows

$$f(x, y) = -\frac{\sin x^2 + y^2}{x^2 + y^2}. \quad (2)$$

The shape of $f(x, y)$ as shown in Figure 4a is similar to a ripple in the water, the initialization point is kept at $(3.0, 3.0)$. We observe that other optimizers get stuck within the ripple of the function, while ours can explore further and eventually find a better minimum.

IV. CONVERGENCE RESULTS

In this section, we prove convergence results. We show that with our choice of learning rate for SGD, our method converges. Moreover, later we also show that the Armijo's condition for our choice learning rate is satisfied.

Theorem 1. *Let $f : \mathbb{R}^n \rightarrow \mathbb{R}$ be a function which is convex and differentiable, and let the gradient of the function be L Lipschitz continuous with Lipschitz constant $L > 0$, i.e., we have that $\|\nabla f(x) - \nabla f(y)\| \leq L\|x - y\|$ then the objective function value will be monotonously decreasing with each iteration of our method.*

Proof. The below equation gives the update rule of our method

$$y = x_t = x_{t-1} - h_{t-1} \cot \theta_{t-1} \frac{\nabla f(x_{t-1})}{\|\nabla f(x_{t-1})\|}. \quad (3)$$

And, let h be constrained as,

$$h_t \leq \frac{\|f(x_t)\|}{L \cot \theta_t}. \quad (4)$$

With assumptions on $f(x)$, we have

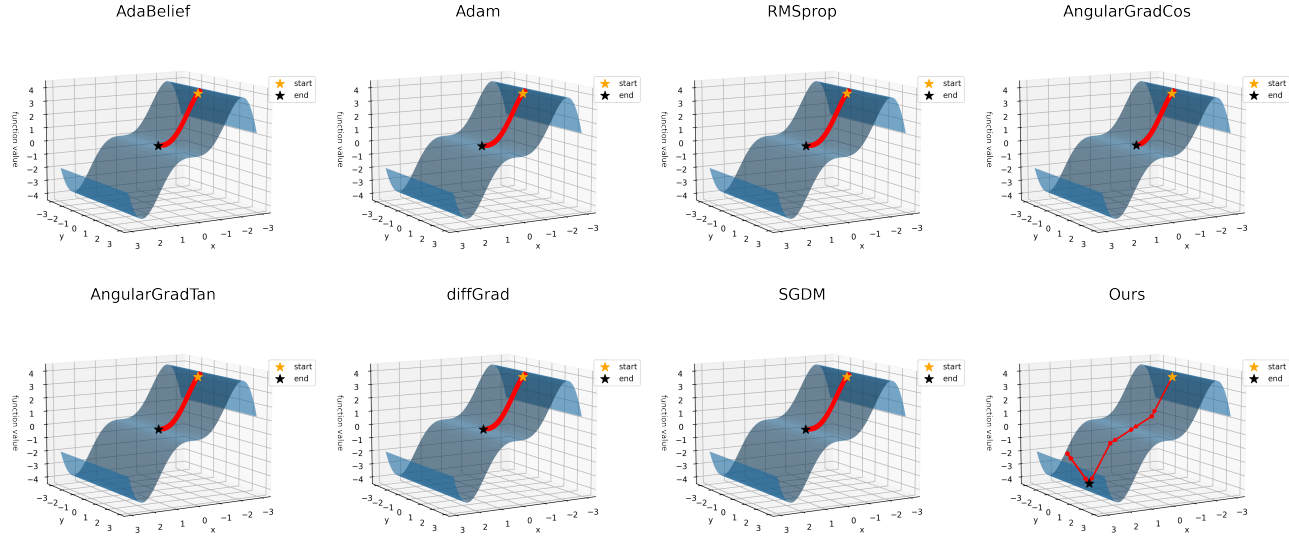
$$f(y) \leq f(x) + \nabla f(x)^T (y - x) + \frac{1}{2} \nabla^2 f(x) \|y - x\|^2.$$

Since $\nabla f(x)$ is L -Lipschitz continuous, $\nabla^2 f(x) \leq L$

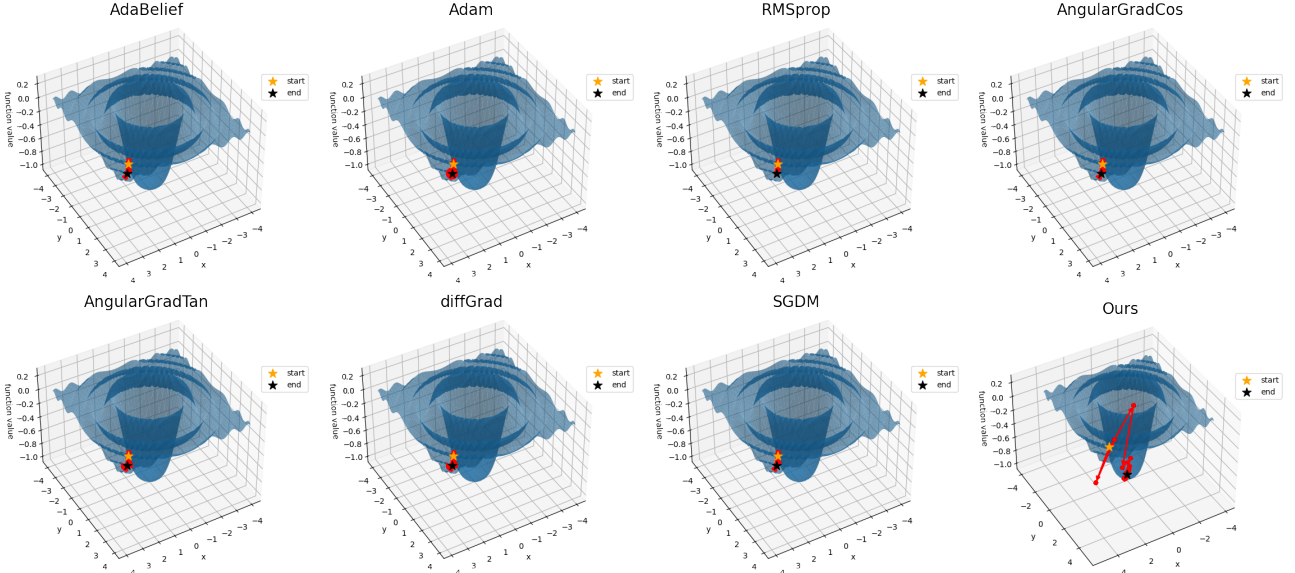
$$f(y) \leq f(x) + \nabla f(x)^T (y - x) + \frac{1}{2} L \|y - x\|^2.$$

Substituting y as in equation 3, and x as x_{t-1} , we get:

$$\begin{aligned} f(x_t) &\leq f(x_{t-1}) + \nabla f(x_{t-1})^T (-h_{t-1} \cot \theta_{t-1} \frac{\nabla f(x_{t-1})}{\|\nabla f(x_{t-1})\|}) \\ &\quad + \frac{1}{2} L \| -h_{t-1} \cot \theta_{t-1} \frac{\nabla f(x_{t-1})}{\|\nabla f(x_{t-1})\|} \|^2 \\ &\leq f(x_{t-1}) + \nabla f(x_{t-1})^T (-h_{t-1} \cot \theta_{t-1} \frac{\nabla f(x_{t-1})}{\|\nabla f(x_{t-1})\|}) \\ &\quad + \frac{1}{2} L h_{t-1}^2 \cot^2 \theta_{t-1} \\ &\leq f(x_{t-1}) + h_{t-1} \cot \theta_{t-1} (\frac{L}{2} h_{t-1} \cot \theta_{t-1} - \|\nabla f(x_{t-1})\|). \end{aligned}$$



(a) Toy Example A: Our method is shown as bottom right figure. We observe that while all other methods get stuck in the local minima, our method can descend further. The black star denotes the terminal point, while the yellow star denotes the starting point.



(a) Toy Example B: Here our method is shown in the bottom right. The black star denotes the terminal point, while the yellow star denotes the starting point. We observe that while all other methods cannot explore efficiently, our method reaches a better local minima.

Using equation 4, we get

$$\begin{aligned} f(x_t) &\leq f(x_{t-1}) + \frac{\|\nabla f(x_{t-1})\|}{L} \left(\frac{\|\nabla f(x_{t-1})\|}{2} - \|\nabla f(x_{t-1})\| \right) \\ &\leq f(x_{t-1}) - \frac{1}{2L} (\|\nabla f(x_{t-1})\|^2). \end{aligned}$$

Hence the objective function decreases with every iterate. \square

A well-known condition on the step length for sufficient decrease in function value is given by Wolfe's condition as stated below. We will show that the first Wolfe's condition, which is Armijo's condition is satisfied, however, we show that second Wolfe's condition is not satisfied.

Theorem 2 (Wolfe's Condition). Let α_k be the step length and p_k be the descent direction for minimizing the function $f(x) : \mathbb{R}^n \rightarrow \mathbb{R}$. Then the strong Wolfe's condition require α_k to satisfy the following two conditions:

$$f(x_k + \alpha_k p_k) \leq f(x_k) + c_1 \alpha_k \nabla f_k^T p_k. \quad (5)$$

$$|\nabla f(x_k + \alpha_k p_k)^T p_k| \leq c_2 |\nabla f_k^T p_k|, \quad (6)$$

with $0 < c_1 < c_2 < 1$.

Proof. See [17, p. 39] for details. \square

Theorem 3 (First Wolfe condition). Under the assumptions

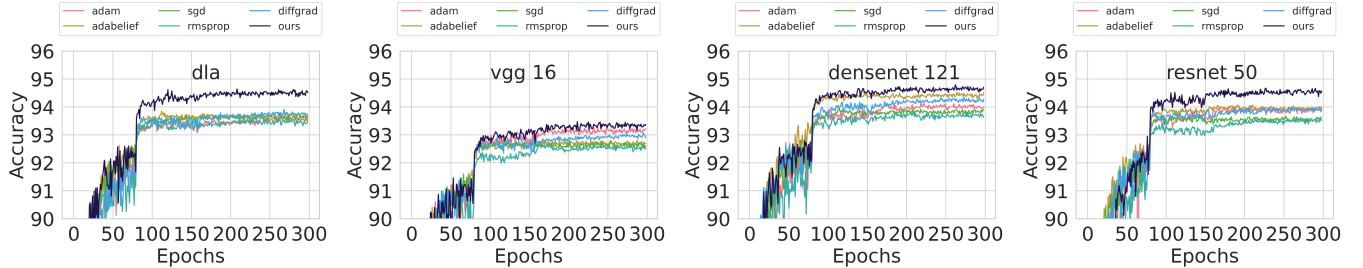


Fig. 5: Accuracy versus epochs plot for image classification for CIFAR-100 results for 300 epochs. We verify that on long term our method maintains high accuracy, and most methods start to stagnate from epochs 100 onwards.

of theorem 1, the update rule in Algorithm 1 satisfies the first Wolfe’s sufficient decrease condition condition (5) with $c_1 = \frac{1}{2L}$.

Proof. We recall that in Wolfe’s conditions, p_k and α are the descent direction and step size, respectively. For our method in Algorithm 1, $p_k = -\nabla f(x_k)$ and $\alpha = h \cot \theta$. From theorem 1 we have the expression,

$$\begin{aligned} f(x_t) &\leq f(x_{t-1}) - \frac{1}{2L}(\|\nabla f(x_{t-1})\|^2) \\ &\leq f(x_{t-1}) + \frac{1}{2L}\nabla f(x_{t-1})^T p_{t-1}. \end{aligned}$$

Hence, for $c_1 = \frac{1}{2L}$ the above inequality holds true. \square

Optimizer	EN-B0	EN-B0 wide	EN-B4	EN-B4 wide
SGD	59.53	59.99	61.45	61.76
ADAM	57.41	55.86	56.20	54.57
RMSPROP	57.98	56.52	57.00	55.77
DIFFGRAD	56.79	56.12	59.03	58.59
AGC	58.61	58.33	58.22	56.46
AGT	58.70	58.08	57.97	56.62
OURS	60.21	60.51	61.32	61.17

TABLE I: Results on mini-ImageNet dataset. Since ImageNet is a relatively large dataset, we have results on EfficientNet only. We observe that our method has the best accuracy for two variants shown in **bold**, and the second best results for the other two variants shown as underlined. Despite hyperparameter tuning, most other methods except vanilla SGD perform poorly.

V. NUMERICAL RESULTS

We test the performance of the current state-of-the-art optimizers with ours on CIFAR-10 [23], CIFAR-100 [23], and mini-imagenet [43].

For CIFAR-10, and CIFAR-100, we take the prominent image classification architectures, these are ResNet18 [11], ResNet34 [11], ResNet50 [11], VGG-16 [37], DLA [45], and DenseNet121 [14], in the tables, we refer to these architectures as RN18, RN34, RN50, VGG16, DLA, and D121 respectively. The current state-of-the-art optimizers are being compared with our method, i.e, Stochastic Gradient Descent with Momentum (SGDM), Adam [21], RMSprop, Adabelief, diffGrad, cosangulargrad (AGC), tanangulargrad (AGT).

Method	RN18	RN34	RN50	D121	VGG16	DLA
SGD	93.18	93.63	93.40	93.85	92.57	93.29
Adam	93.85	93.99	93.88	94.28	92.66	93.57
RMSProp	93.63	<u>94.07</u>	93.42	93.84	92.36	93.29
AdaBelief	93.57	93.71	93.80	94.26	<u>92.84</u>	93.72
diffGrad	93.85	93.73	93.65	94.28	92.67	93.49
AGC	93.64	94.02	94.05	<u>94.57</u>	92.64	93.6
AGT	<u>93.92</u>	93.89	<u>94.11</u>	94.50	92.76	<u>93.74</u>
OURS	94.00	94.24	94.39	94.75	93.18	94.38

TABLE II: Overall accuracies on CIFAR-10 first 100 epochs. The best results are in **bold**, and second best is underlined. We find that our method has the best accuracy among all the methods compared. Here RN stands for ResNet, D121 is DenseNet-121, and DLA is Deep Layer Aggregation.

To see long term result and stagnation of accuracy for CIFAR-100, a relatively large dataset, we run for 300 epochs and show accuracy results in Figure 5 for ResNet50, VGG-16, DenseNet-121, and DLA. Our method performs substantially better on DLA, and achieves best accuracy for resnet-50 and DenseNet on CIFAR-100.

Figure 6 shows accuracy versus epochs for CIFAR-10 for 3 runs and hence variations are seen around mean; we show the mean by bold lines. The best accuracy results for CIFAR-10 dataset are also shown in Table II. We observe that our method performs the best across all the architectures; with more pronounced accuracy for the DLA and VGG. The observed jump in performance at epoch 80 is due to the learning rate scheduler, which is set to reduce the learning rate by 10 at the 80th epoch. The ablation study of our method on CIFAR-10 is further described in the supplementary.

The experimental results for CIFAR-100 are shown in the Table III, and the plots for accuracy versus epochs for multiple runs are shown in the Figure 7. We perform the best in most of the architectures, except on ResNet-50 and our method performs the second best for VGG-16.

Mini-imagenet [44] dataset is a subset of the large Imagenet dataset [6]. We use the efficient net architecture for mini-imagenet because as shown in Figure 1 in the paper [41], efficient-net provides the best accuracy per parameter. The best accuracy results of the mini-imagenet is shown in Table I. We outperform all the standard state-of-the-art methods that use decaying expectations of the gradient terms (includes

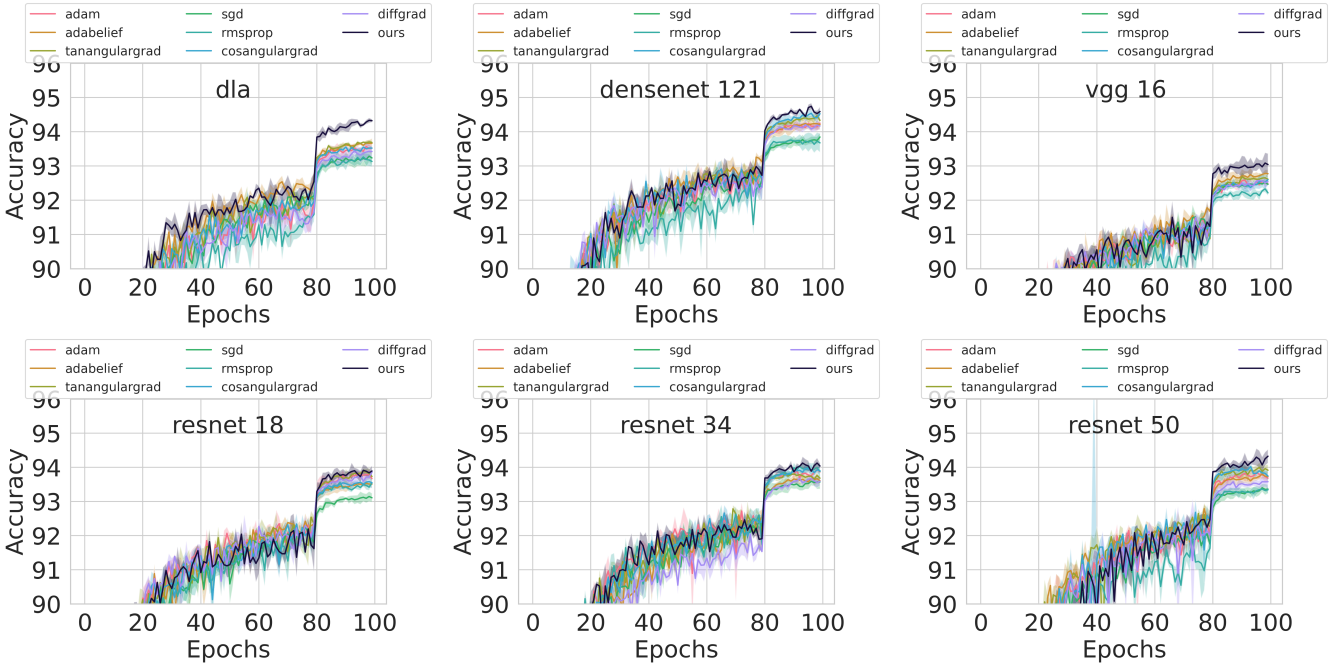


Fig. 6: Accuracy plots versus epochs for image classification on the CIFAR-10 dataset. Our method is represented by dark purple curve, which is an average over 3 runs. The variance observed is not much around the mean. On DLA we observe a significantly better accuracy. On other architectures, our method maintains the highest accuracy.

momentum based methods) to either scale the gradient or correct its direction. We perform best in EfficientNet-B0 and EfficientNet-B0 wide; second best in EfficientNet-B4 and EfficientNet-B4 wide while performing substantially better than the adaptive methods.

Method	RN18	RN34	RN50	D121	VGG16	DLA
SGD	72.94	73.31	73.82	74.82	69.24	73.84
Adam	71.98	71.92	73.52	74.50	67.78	71.33
RMSProp	68.90	69.66	71.13	71.74	65.79	67.91
AdaBelief	73.07	73.44	<u>75.47</u>	<u>75.60</u>	69.63	<u>74.09</u>
diffGrad	72.02	72.21	74.08	74.53	67.83	71.07
AGC	<u>73.25</u>	<u>73.64</u>	75.46	75.36	69.21	72.84
AGT	73.13	73.35	75.75	75.39	68.85	73.06
OURS	73.33	74.22	74.44	76.79	69.46	74.92

TABLE III: Overall accuracies on CIFAR-100 first 100 epochs. The best results are shown in **bold**, and the second best results are underlined. We observe that our method has the best results on four architectures and the second best on one architecture. Here RN stands for ResNet, D121 is DenseNet-121, and DLA is Deep Layer Aggregation.

VI. CODE REPOSITORY

<https://github.com/misterpawan/dycent>.

VII. CONCLUSION

We propose a simple and novel method for finding an adaptive learning rate for stochastic gradient-based descent methods for image classification tasks on prominent and recent convolution neural networks such as ResNet, VGG,

DenseNet, EfficientNet. We observe that the proposed learning rate leads to higher accuracy compared to existing state-of-the-art methods such as AdaBelief, Adam, SGD, RMSProp, diffGrad, etc. We also show that the proposed learning rate leads to convergence and satisfies one of the Wolfe's condition also called Armijo's condition. The advantages of the proposed method is in change in learning rate which is found geometrically, and it is better than more costly momentum-based methods. Our future plans include analyzing and extending our method to other architectures and applications and expanding the theory to non-convex cases with a specific emphasis on improving the convergence rate.

ACKNOWLEDGEMENT

This work was funded by Microsoft Academic Partnership Grant (MAPG), IHUB at IIIT, and Qualcomm Faculty Award at IIIT, Hyderabad, India. We acknowledge the support of the host institute for compute resources.

REFERENCES

- [1] Michele Benzi. Preconditioning techniques for large linear systems: A survey. *Journal of Computational Physics*, 182(2):418–477, 2002.
- [2] David E Carlson, Edo Collins, Ya-Ping Hsieh, Lawrence Carin, and Volkan Cevher. Preconditioned spectral descent for deep learning. In C. Cortes, N. Lawrence, D. Lee, M. Sugiyama, and R. Garnett, editors, *Advances in Neural Information Processing Systems*, volume 28. Curran Associates, Inc., 2015.
- [3] Shruti Das, Siddhant Katyan, and Pawan Kumar. Domain decomposition based preconditioned solver for bundle adjustment. In R. Venkatesh Babu, Mahadeva Prasanna, and Vinay P. Namboodiri, editors, *Computer Vision, Pattern Recognition, Image Processing, and Graphics*, pages 64–75, Singapore, 2020. Springer Singapore.

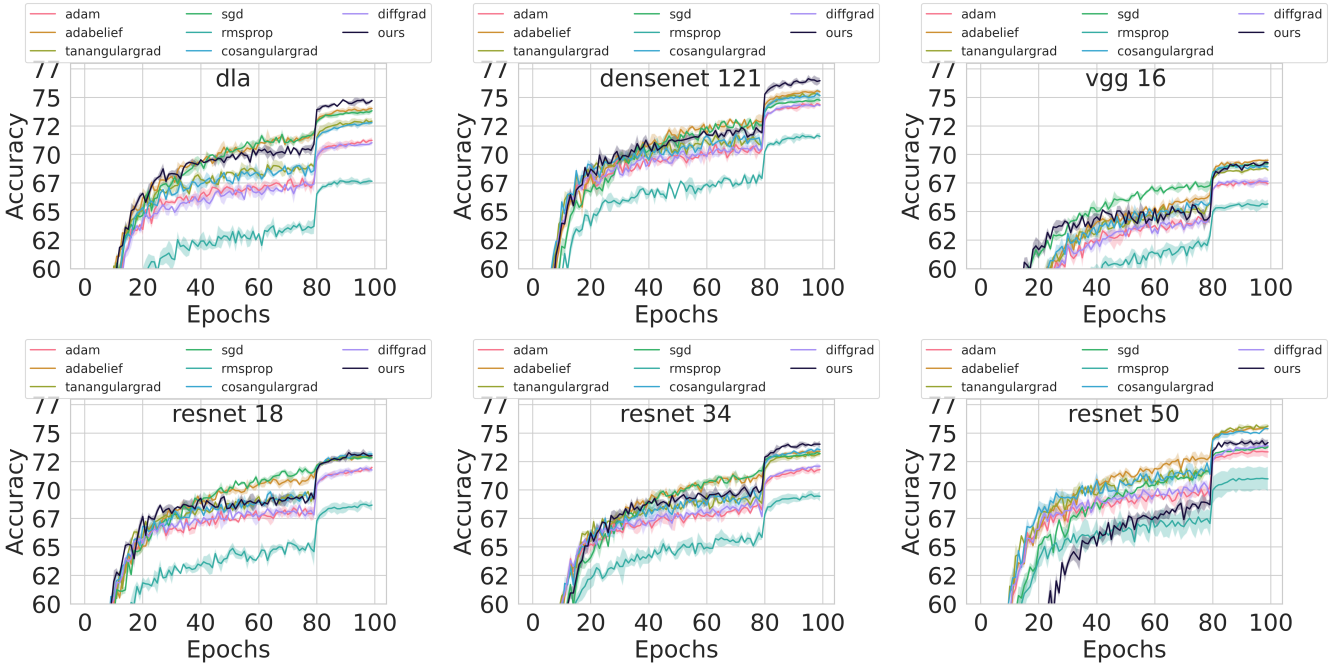


Fig. 7: Accuracy plots versus epochs for image classification on CIFAR-100 dataset. Our method is represented by dark purple curve. Except for ResNet50 and VGG16, our method achieves the highest accuracy. The accuracy plots for longer number of epochs is shown in Figure 5. For hyper-parameters and ablation study, please refer to supplementary material.

- [4] Shrutimoy Das, Siddhant Katyan, and Pawan Kumar. A deflation based fast and robust preconditioner for bundle adjustment. In *Proceedings of the IEEE/CVF Winter Conference on Applications of Computer Vision (WACV)*, pages 1782–1789, January 2021.
- [5] Arpan Dasgupta, Siddhant Katyan, Shrutimoy Das, and Pawan Kumar. Review of extreme multilabel classification, 2023.
- [6] Jia Deng, Wei Dong, Richard Socher, Li-Jia Li, Kai Li, and Li Fei-Fei. Imagenet: A large-scale hierarchical image database. In *2009 IEEE Conference on Computer Vision and Pattern Recognition*, pages 248–255, 2009.
- [7] Timothy Dozat. Incorporating nesterov momentum into adam. *ICLR Workshop*, 1:2013–2016, 2016.
- [8] Shiv Ram Dubey, Soumendu Chakraborty, Swalpa Kumar Roy, Snehasis Mukherjee, Satish Kumar Singh, and Bidyut Baran Chaudhuri. diffgrad: an optimization method for convolutional neural networks. *IEEE transactions on neural networks and learning systems*, 31(11):4500–4511, 2019.
- [9] John Duchi, Elad Hazan, and Yoram Singer. Adaptive subgradient methods for online learning and stochastic optimization. *Journal of machine learning research*, 12(7), 2011.
- [10] Ian J. Goodfellow, Yoshua Bengio, and Aaron Courville. *Deep Learning*. MIT Press, Cambridge, MA, USA, 2016. <http://www.deeplearningbook.org>.
- [11] Kaiming He, Xiangyu Zhang, Shaoqing Ren, and Jian Sun. Deep residual learning for image recognition. In *Proceedings of the IEEE conference on computer vision and pattern recognition*, pages 770–778, 2016.
- [12] Byeongho Heo, Sanghyuk Chun, Seong Joon Oh, Dongyo Han, Sangdoo Yun, Gyuwon Kim, Youngjung Uh, and Jung-Woo Ha. Adamp: Slowing down the slowdown for momentum optimizers on scale-invariant weights. *arXiv preprint arXiv:2006.08217*, 2020.
- [13] Geoffrey Hinton, Nitish Srivastava, and Kevin Swersky. Neural networks for machine learning lecture 6a overview of mini-batch gradient descent. *Lecture notes from University of Toronto*, 14(8):2, 2012.
- [14] Gao Huang, Zhuang Liu, Laurens van der Maaten, and Kilian Q. Weinberger. Densely connected convolutional networks, 2016.
- [15] Haiwen Huang, Chang Wang, and Bin Dong. Nostalgic adam: Weighting more of the past gradients when designing the adaptive learning rate. *arXiv preprint arXiv:1805.07557*, 2018.
- [16] Ben Joffe. Functions 3d: Examples. <https://www.benjoffe.com/code/tools/functions3d/examples>.
- [17] Stephen J. Wright Jorge Nocedal. *Numerical Optimization*. Springer-Verlag, New York, 2006.
- [18] Siddhant Katyan, Shrutimoy Das, and Pawan Kumar. Two-grid preconditioned solver for bundle adjustment. In *2020 IEEE Winter Conference on Applications of Computer Vision (WACV)*, pages 3588–3595, 2020.
- [19] Pawan Kumar Kinal Mehta, Anuj Mahajan. Effects of spectral normalization in multi-agent reinforcement learning. In *IJCNN*, 2023.
- [20] Diederik P Kingma and Jimmy Ba. Adam: A method for stochastic optimization. *arXiv preprint arXiv:1412.6980*, 2014.
- [21] Diederik P. Kingma and Jimmy Ba. Adam: A method for stochastic optimization, 2014.
- [22] Stefan Klein, Marius Staring, Patrik Andersson, and Josien P. W. Pluim. Preconditioned stochastic gradient descent optimisation for monomodal image registration. In Gabor Fichtinger, Anne Martel, and Terry Peters, editors, *Medical Image Computing and Computer-Assisted Intervention – MICCAI 2011*, pages 549–556, Berlin, Heidelberg, 2011. Springer Berlin Heidelberg.
- [23] Alex Krizhevsky, Vinod Nair, and Geoffrey Hinton. Cifar-10, and cifar-100 (canadian institute for advanced research).
- [24] Pawan Kumar. Aggregation based on graph matching and inexact coarse grid solve for algebraic two grid. *International Journal of Computer Mathematics*, 91(5):1061–1081, 2014.
- [25] Pawan Kumar, L. Grigori, F. Nataf, and Q. Niu. On relaxed nested factorization and combination preconditioning. *International Journal of Computer Mathematics*, 93(1):179–199, 2016.
- [26] Pawan Kumar, Stefano Markidis, Giovanni Lapenta, Karl Meerbergen, and Dirk Roose. High performance solvers for implicit particle in cell simulation. *Procedia Computer Science*, 18:2251–2258, 2013. 2013 International Conference on Computational Science.
- [27] Pawan Kumar, Karl Meerbergen, and Dirk Roose. Multi-threaded nested filtering factorization preconditioner. In Pekka Manninen and Per Öster, editors, *Applied Parallel and Scientific Computing*, pages 220–234, Berlin, Heidelberg, 2013. Springer Berlin Heidelberg.
- [28] Liyuan Liu, Haoming Jiang, Pengcheng He, Weizhu Chen, Xiaodong Liu, Jianfeng Gao, and Jiawei Han. On the variance of the adaptive learning rate and beyond. *arXiv preprint arXiv:1908.03265*, 2019.

- [29] Pratik Mandrecha, Snehit Kumar Chatakonda, Neeraj Kollepara, and Pawan Kumar. *Hybrid Tokenization and Datasets for Solving Mathematics and Science Problems Using Transformers*, pages 289–297. SIAM, 2022.
- [30] I. Mishra, A. Dasgupta, B. Mishra, P. Jawanpuria, and Pawan. Kumar. Light-weight deep extreme multilabel classification. In *IJCNN*, 2023.
- [31] Yurii Evgen'evich Nesterov. A method of solving a convex programming problem with convergence rate $o(k^2)$. In *Doklady Akademii Nauk*, pages 372–367. Russian Academy of Sciences, 1983.
- [32] Ning Qian. On the momentum term in gradient descent learning algorithms. *Neural Networks*, 12(1):145–151, 1999.
- [33] M. Riedmiller and H. Braun. A direct adaptive method for faster backpropagation learning: the rprop algorithm. In *IEEE International Conference on Neural Networks*, pages 586–591 vol.1, 1993.
- [34] SK Roy, ME Paoletti, JM Haut, SR Dubey, P Kar, A Plaza, and BB Chaudhuri. Angulargrad: A new optimization technique for angular convergence of convolutional neural networks. *arXiv preprint arXiv:2105.10190*, 2021.
- [35] Sebastian Ruder. An overview of gradient descent optimization algorithms. *arXiv preprint arXiv:1609.04747*, 2016.
- [36] Yousef Saad. *Iterative Methods for Sparse Linear Systems*. Society for Industrial and Applied Mathematics, Philadelphia, PA, USA, 2 edition, 2003.
- [37] Karen Simonyan and Andrew Zisserman. Very deep convolutional networks for large-scale image recognition, 2014.
- [38] Chongya Song, Alexander Pons, and Kang Yen. Ag-sgd: Angle-based stochastic gradient descent. *IEEE Access*, 9:23007–23024, 2021.
- [39] Ilya Sutskever, James Martens, George Dahl, and Geoffrey Hinton. On the importance of initialization and momentum in deep learning. In *International conference on machine learning*, pages 1139–1147. PMLR, 2013.
- [40] Richard S. Sutton and Andrew G. Barto. *Reinforcement Learning: An Introduction*. The MIT Press, second edition, 2018.
- [41] Mingxing Tan and Quoc Le. Efficientnet: Rethinking model scaling for convolutional neural networks. In *International conference on machine learning*, pages 6105–6114. PMLR, 2019.
- [42] Ashish Vaswani, Noam Shazeer, Niki Parmar, Jakob Uszkoreit, Llion Jones, Aidan N Gomez, Łukasz Kaiser, and Illia Polosukhin. Attention is all you need. In *Advances in Neural Information Processing Systems*, pages 5998–6008, 2017.
- [43] Oriol Vinyals, Charles Blundell, Timothy Lillicrap, koray kavukcuoglu, and Daan Wierstra. Matching networks for one shot learning. In D. Lee, M. Sugiyama, U. Luxburg, I. Guyon, and R. Garnett, editors, *Advances in Neural Information Processing Systems*, volume 29. Curran Associates, Inc., 2016.
- [44] Oriol Vinyals, Charles Blundell, Timothy Lillicrap, Daan Wierstra, et al. Matching networks for one shot learning. *Advances in neural information processing systems*, 29, 2016.
- [45] Fisher Yu, Dequan Wang, Evan Shelhamer, and Trevor Darrell. Deep layer aggregation. In *2018 IEEE/CVF Conference on Computer Vision and Pattern Recognition*, pages 2403–2412, 2018.
- [46] Matthew D Zeiler. Adadelta: an adaptive learning rate method. *arXiv preprint arXiv:1212.5701*, 2012.
- [47] Juntang Zhuang, Tommy Tang, Yifan Ding, Sekhar C Tatikonda, Nicha Dvornek, Xenophon Papademetris, and James Duncan. Adabelief optimizer: Adapting stepsizes by the belief in observed gradients. *Advances in neural information processing systems*, 33:18795–18806, 2020.